A HIGH RESOLUTION SIMULATION OF THE WIND- AND THERMOHALINE-DRIVEN CIRCULATION IN THE NORTH ATLANTIC OCEAN

Frank O. Bryan and William R. Holland

National Center for Atmospheric Research, P.O. Box 3000, Boulder, Colorado, 80307

ABSTRACT

A simulation of the general circulation of the North Atlantic Ocean has been carried out using a thermodynamic primitive equation numerical model with sufficient horizontal resolution to explicitly include the hydrodynamic instability processes responsible for eddy formation. The model is forced with climatological, seasonally varying, wind stress and surface heat and salt fluxes. The role of eddies in the general circulation, including their interactions with thermodynamic processes such as poleward heat transport and thermocline ventilation are being investigated. While the simulation has some obvious deficiencies, the overall quality of the solution is very good, leading us to believe that the next level of model development should be directed at more accurate representations of diapycnal processes and the incorporation of more realistic surface forcing.

INTRODUCTION

The ubiquity of mesoscale motions and their importance in the general circulation are well established facts in oceanography. The role that ocean eddies play in global climate is still an open question however. The sparsity of current measurements precludes direct estimates of the eddy contribution in basin- to global-scale heat budgets. The dichotomy that has existed in ocean modeling over the last decade has also prevented us from answering this question. On one hand are models with active thermodynamics and moderate to high vertical resolution, but low horizontal resolution. These have been developed in an attempt to represent the large-scale hydrographic structure and climatic properties (water mass formation rates, heat and freshwater transports, sea surface temperature anomalies, etc.) of individual ocean basins or the world ocean. The strong dissipation required to maintain numerical stability in these low resolution models inhibits physically realistic hydrodynamic instabilities as well. Thus, the only source of variability in this type of simulation is time dependence in the imposed atmospheric forcing (or open boundary conditions if they exist). This class of models has been moderately successful in simulating the mean circulation and hydrographic structure of the world ocean, e.g., Bryan (1979), Meehl et al. (1982), and the variability of the upper ocean circulation where the variability is primarily wind forced, e.g., Sarmiento (1986), Philander et al. (1987). On the other hand are models with high horizontal resolution, but low vertical resolution, and generally incomplete treatment of thermodynamic processes. These have been developed in order to investigate the dynamics of time-dependent circulation systems including mesoscale eddies and their interactions with the mean flow. This class of models has shown some success in representing the distributions of eddy variability and the structure of western boundary currents of the

subtropical gyre circulations systems, e.g., Holland et al. (1983), Holland (1985, 1986). Studies carried out with these models have provided insights leading to major advances in the theory of the ocean general circulation. The majority of these calculations have been carried out using the quasigeostrophic equation system. This system does not contain the high frequency gravity waves, and is hence much more economical to integrate than the primitive equation system. However, thermohaline processes are difficult to incorporate into these models and they are limited to non-global domains.

The advent of the current generation of supercomputers has facilitated the convergence of these two modeling approaches. Basin- to global-scale simulations which include both a complete representation of the thermodynamic processes responsible for water mass formation and sufficient horizontal resolution to allow the hydrodynamic instabilities responsible for eddy formation have become feasible. In this paper we describe such a calculation for the circulation in the North Atlantic basin. In addition to addressing basic questions about the role of mesoscale motions in the ocean general circulation and climate, this experiment is meant to serve as a benchmark to judge our progress in basin-scale modeling. The results of this experiment and their analysis will help guide future development efforts by indicating which aspects of the models are most in need of improvement and which are most successful and by providing a reference solution against which to compare succesive experiments. These analyses are still underway, so only a preliminary overview of the results will be presented here.

MODEL CONFIGURATION

The basic model used in this experiment is the primitive equation model developed at the NOAA Geophysical Fluid Dynamics Laboratory by Bryan (1969) and Cox (1984). This model has been used extensively for a variety of ocean modeling problems. The equations of motion are formulated using second-order finite-differences on the Arakawa B-grid (Arakawa and Lamb, 1977) and conserve total heat content (or arbitrary scalar tracer content), mass, energy, and tracer variance in the absence of explicit dissipation or forcing. The horizontal resolution is 1/3° in latitude and 2/5° in longitude. This gives equal grid spacing in the north-south and east-west directions of 37 km at 34° latitude. Note that this is approximately equal to the radius of deformation for the first baroclinic mode in mid-latitudes, so that the resolution is just barely adequate to represent many of the eddying processes. There are 30 discrete levels in the vertical, with a spacing of 35 m at the surface and smoothly stretching to 250 m by 1000 m depth. Below 1000 m the vertical grid spacing is a constant 250 m. The computational domain is the North Atlantic basin from 15°S to 65°N latitude, including the Caribbean Sea and Gulf of Mexico, but excluding the Mediterranean Sea (Figure 1). Cuba and Hispañola are treated as true islands, requiring special treatment of the boundary conditions on the barotropic streamfunction. Bottom topography is represented in the model as stacked grid boxes, so that the bottom lies on the interface between two grid levels. The topography is derived from a digital terrain data set with 5' latitude-longitude resolution using a simple nearest neighbor approach. The only smoothing performed is to remove single grid point holes or spikes.

Since this is the first experiment of its kind, we had little guidance in choosing parameterization schemes. Several criteria were considered when making these choices. First, we wanted this experiment to represent the state-of-the art in general circulation modeling. As this is to be the first experiment in a series and will provide a reference

point for comparing future solutions, it was desirable to keep the parameterizations in this initial experiment fairly simple. The horizontal dissipation mechanism is a highly scale-selective, biharmonic operator with a coefficient of -2.5×10^{19} cm^4s^{-1} for both momentum and tracers. The vertical dissipation mechanism is the more traditional second order operator with constant coefficients of 30 cm^2s^{-1} for momentum and 0.3 cm^2s^{-1} for tracers. Additional dissipation of momentum is provided by a quadratic bottom drag. A Kraus-Turner type, surface mixed-layer parameterization is included as a purely vertical process, that is, there is no horizontal communication of mixed-layer depth or turbulence levels between adjacent grid points. A conventional adjustment scheme is used to treat free convective mixing.

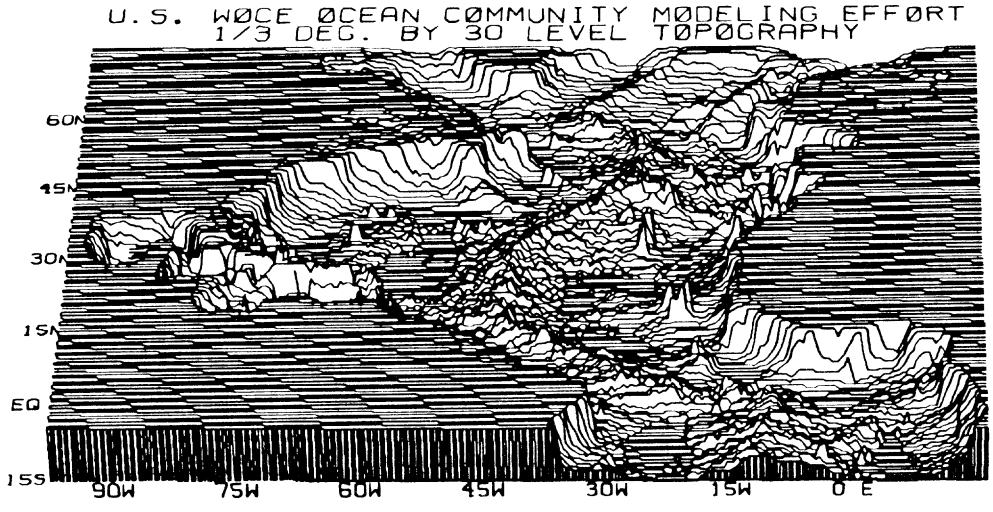

Figure 1. Three-dimensional perspective view of the bottom topography used in the experiment.

The surface boundary conditions are all based on seasonal climatological data sets. The wind stress and wind work values are taken from the Hellerman and Rosenstein (1983) climatology. The surface thermal boundary conditions are specified by a linear bulk formula described by Han (1984). In this scheme the heat flux is a linear function of the difference between the model-predicted, sea surface temperature and a prescribed "effective" atmospheric temperature that includes corrections for effects like direct solar radiation. The proportionality coefficient varies temporally and spatially, and is primarily a function of surface wind speed. Due to the lack of reliable data sets for precipitation over the ocean, the surface boundary condition for fresh water flux is implemented as a linear damping of salinity in the first model level towards the Levitus (1982) seasonal climatology. Linear interpolation between monthly or seasonal means is used to obtain necessary values for all surface forcing fields at each model time step.The restriction of the model domain to a less than global one decreases the computational burden considerably but introduces the complication of open boundaries. In this experiment these are treated by closing the boundaries to inflow or outflow but introducing narrow "buffer zones" adjacent to them. In these buffer zones the temperature and salinity are damped towards their (seasonally varying) climatological values on a time scale of 25 days at the outer edge (approximately 150 km from the

walls), linearly decreasing to 5 days adjacent to the wall. The damping terms in these buffer zones must provide the heat and salt sources and, for example, sinks to convert southward flowing North Atlantic Deep Water to northward flowing surfaces waters at the southern boundary.

The experiment was initialized with temperature and salinity for January conditions from the Levitus (1982) climatology. Due to the rather strong smoothing used to construct this data set, a number of frontal features are seriously distorted in the initial condition. For example, the cold slope water north of the Gulf Stream west of 40°W is almost completely missing from the initial condition.

The model contains over two million grid points, and requires approximately 50 Cray XMP CPU hours for each year of integration. The evolving model solution was sampled at three-day intervals during the final five years of the simulation. The resulting archive of 600 samples requires over 50 Gigabytes of mass storage. Regional and temporal subsamples of the archive, as well as various statistics derived from it, are being made available to interested investigators.

RESULTS

The complexity of the solution and the volume of data required to describe it prevent a thorough description of the results in any single paper. Indeed, many investigators are involved in the analysis of this experiment since such a wide variety of phenomena are represented in the solution. In this section we will give an overview of the largest scale features of the circulation and some of the processes relevant to the climate problem.

Mean Circulation, Water Masses and Variability

During the relatively short integration, there is little drift of the basic hydrographic structure away from that described by the initial conditions. The level mean temperatures for depths less than 2000 m warm slightly during the integration, and those below 2000 m cool slightly. The mean, sea surface temperature (SST) for January over the last 15 years of the simulation is shown in Figure 2a, and the difference between the model January mean SST and the Levitus (1982) climatology is shown in Figure 2b. Over most of the basin, the model differs from the climatology by less than 1°C. The largest differences are found in the Gulf Stream region. The model Gulf Stream is displaced to the north of the mean observed position between 50°W and 75°W. This results in large positive differences on the inshore side of the Gulf Stream. The differences between the climatological SST's and the model predictions for other months show similar patterns. A 1° resolution version of the model has a similar pattern as well, with the exception that the region of anomalously warm SST along the western boundary has a larger areal extent. This is an indication that surface temperatures and heat storage away from regions of strong currents are determined primarily by local vertical processes, as suggested by Gill and Niiler (1973), and that the specification of the surface heat flux and mixed layer parameterization in the model are reasonably accurate.

The model is also successful in simulating the formation of both subtropical and subpolar mode waters. Meridional temperature sections in the upper layers of the western basin are shown in Figure 3 for January and July during the final year of the integration. During winter the mixed layer extends to 300 m depth on the south side of

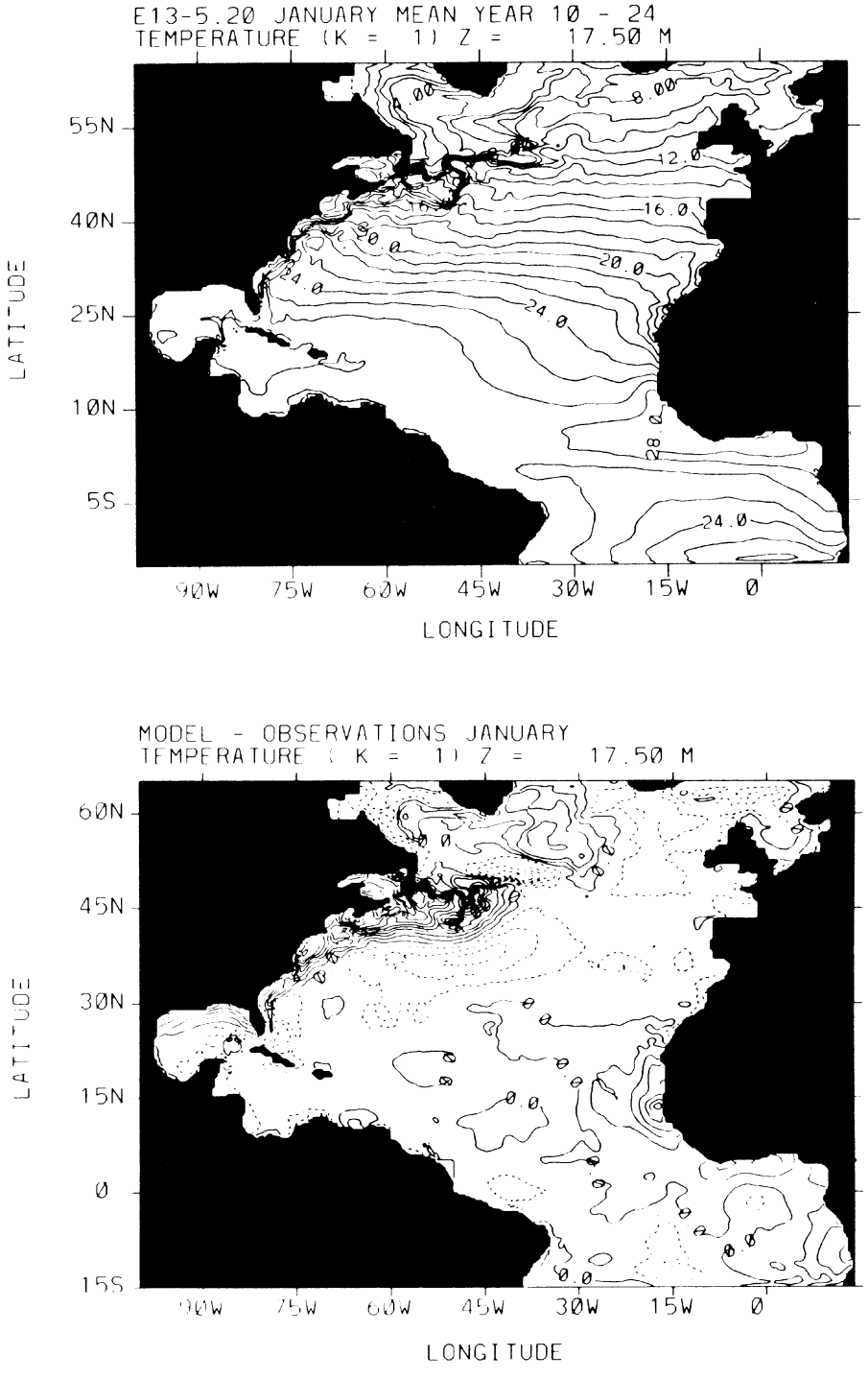

Figure 2. (a) Mean January sea surface temperature from the final 15 years of the experiment. (b) Difference between the model mean January sea surface temperatures and the Levitus (1982) January climatology.

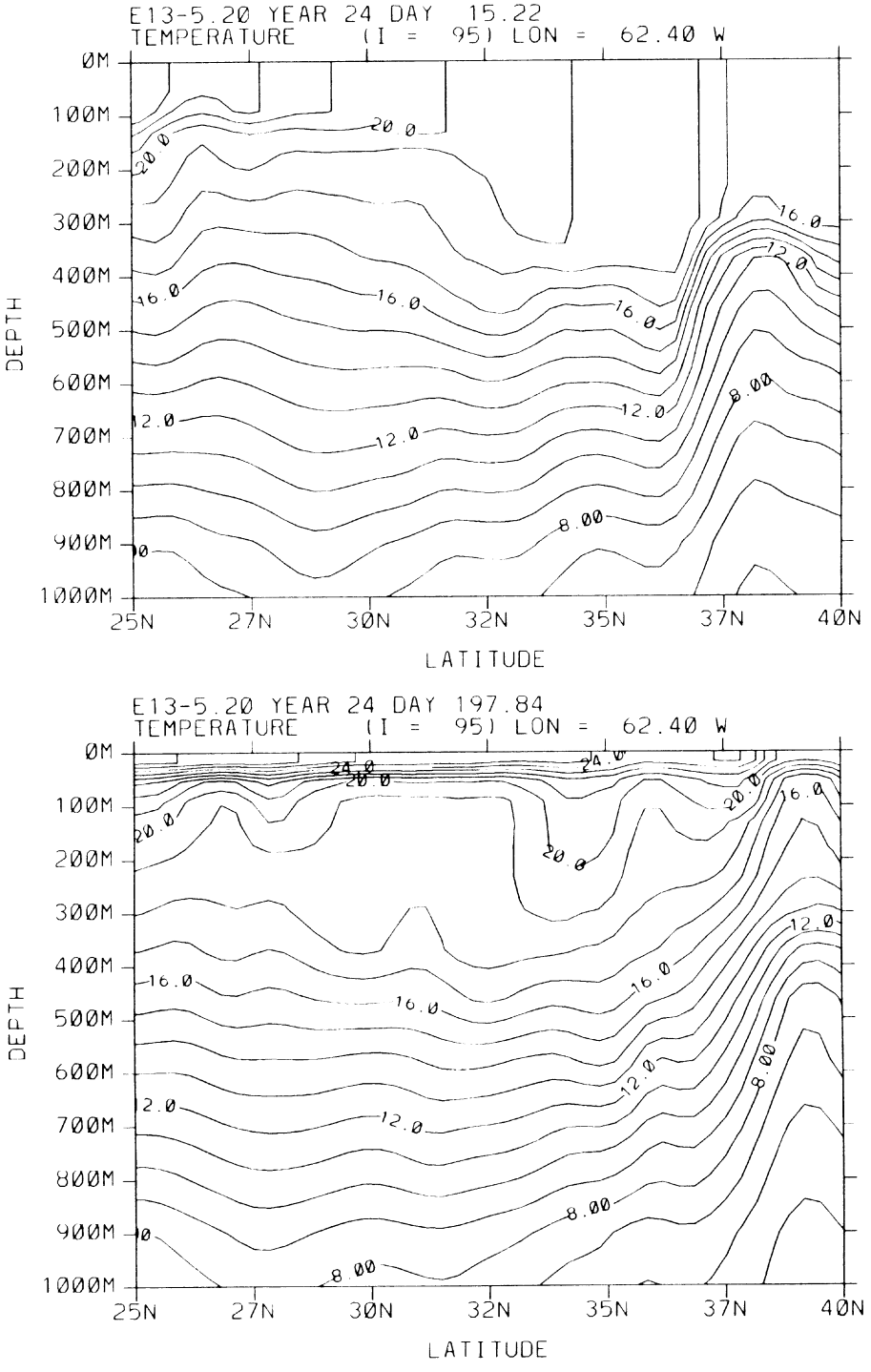

Figure 3. (a) Meridional temperature section in the upper 1000 m along 62.4°W longitude for mid-January during the last year of the experiment. (b) As in (a) for mid-July.

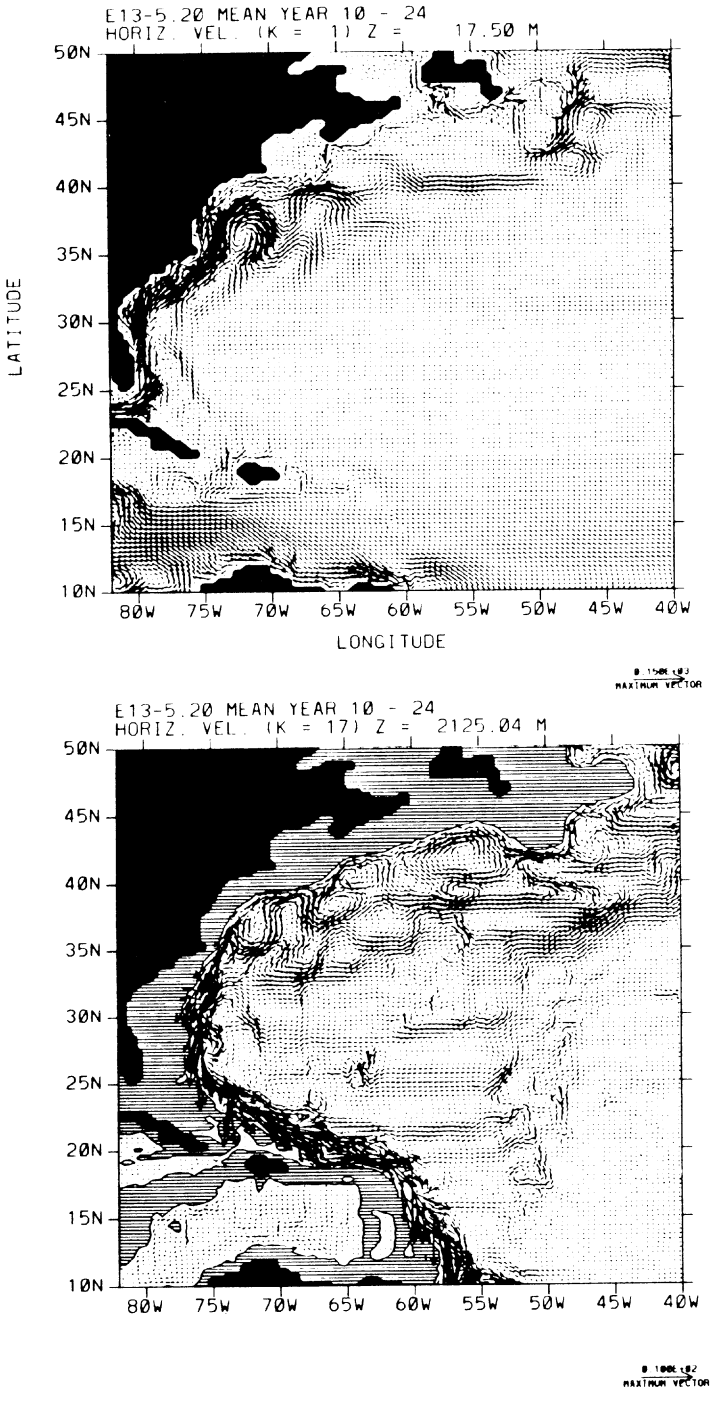

Figure 4. (a) Mean horizontal velocity at the first model level (17.5 m) for January. Vector in the lower right represents 150 cm s^{-1}. (b) Mean horizontal velocity at 2125 m for January. Vector in the lower right represents 10 cm s^{-1}. Areas with cross hatching indicate topography shallower than 2250 m.

the Gulf Stream (36° to 37°N). During summer, a seasonal thermocline forms at approximately 50 m depth, leaving behind a thick layer of 18° water, or subtropical mode water. This process is the primary ventilation mechanism in the western part of the basin. A second distinct mode water with a temperature around 12°C forms further east along the North Atlantic Current, and a subpolar mode water with a temperature around 4°C forms in the Labrador Sea.

The shifted position of the Gulf Stream is apparent in the January mean surface currents shown in Figure 4a. Whereas the Gulf Stream is observed to separate from the coast at Cape Hatteras, in the model it follows the coast for several hundred kilometers further north. The separation in the model is dominated by a very tight and nearly stationary anticyclonic gyre that is not observed in reality. This type of error in the western boundary current separation region is common in experiments with primitive equation models, yet the dynamical processes involved are still unclear. The lack of a strong theoretical understanding of the physics of boundary current separation compounds the difficulty of trying to understand this aspect of the model solution. South of Cape Hatteras the simulation of the western boundary current is much more realistic. The mean barotropic transport just south of Cape Hatteras is approximately 50 Sverdrups. The core of the southward flowing North Atlantic Deep Water is located between 2000 and 3000 m depth. As shown in Figure 4b, a coherent deep western boundary current can be identified everywhere south of Cape Hatteras. Between Cape Hatteras and the Grand Banks, a weaker westward flow can be seen following the continental slope. In any instantaneous realization the flow at this level, north and east of Cape Hatteras, is dominated by the eddy field.

The time series for the volume transport through the Florida Straits is shown in Figure 5. The well-documented seasonal variation of the transport (see Leaman et al., 1987), with a maximum in summer and a sharp drop in fall, is reproduced by the model. Both the amplitude and the phase of the variability agree well with the observations. The model solution also shows a large amount of interannual variability. The annual mean transport is somewhat too low however. This is not too surprising, given that the model resolves the Florida Straits with only three grid points in the zonal direction.

With the emergence of satellite altimetry it has become possible to accurately map the distribution of eddy variability in the ocean. This provides one of the few basin- to global-scale measurements of variability with which to compare the models. The distribution of the standard deviation of the surface elevation in the model is shown in Figure 6. The peak values in the Gulf Stream region are approximately 30 cm. This compares favorably with the estimates of Koblinsky (1988) derived from the GEOSAT altimeter. The secondary maximum in variability off the coast of Brazil is also reproduced by the model. The sea level variability in the interior, away from the western boundary, is too low by a factor of two however. This may be due to the lack of subseasonal frequencies in the wind forcing.

Heat Transport and Meridional Circulation

A primary quantity of climatic interest is the poleward heat transport and, especially for this study, the contribution of the eddies. The mean seasonal cycle of the total northward heat transport is shown in Figure 7. The most prominent signal is the large variability in the tropics, where the heat transport reaches a maximum of 1.3×10^{15} W in January and a minimum of -0.7×10^{15} W in August. This is associated with the

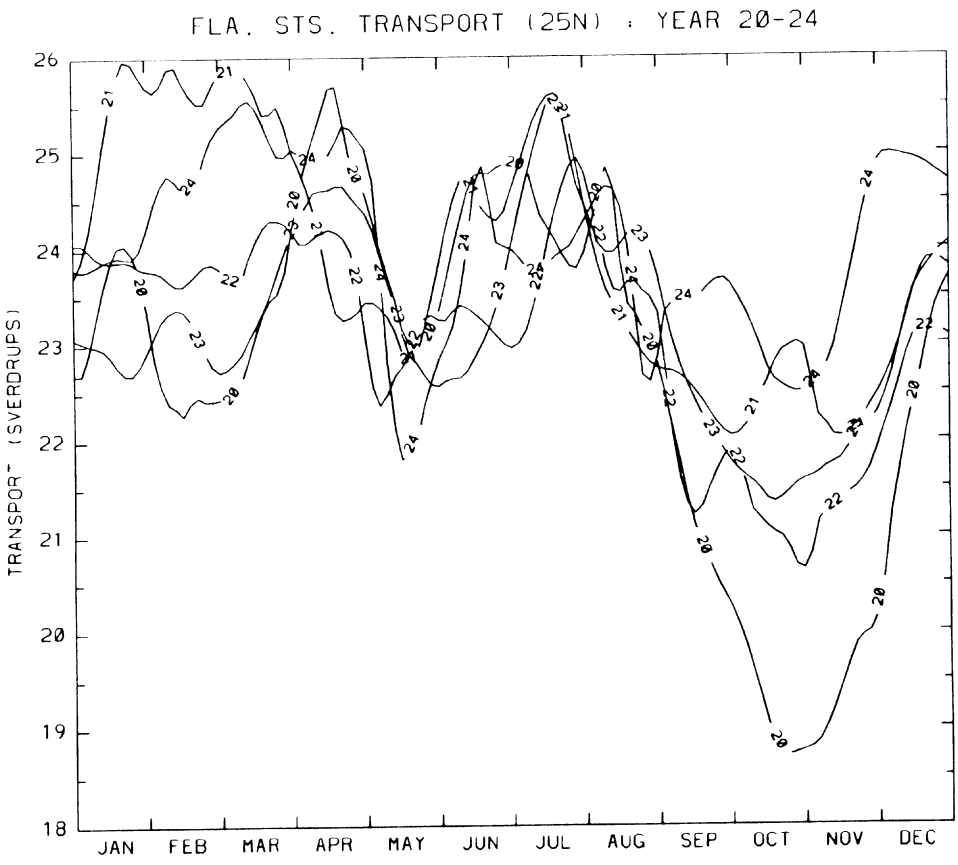

Figure 5. Barotropic transport in the Florida Straits during the final 5 years of the experiment.

seasonal onset of the North Equatorial Counter Current, as discussed below. The annual mean transport reaches a maximum of 0.6×10^{15} W at 35°N latitude. Hall and Bryden (1982) estimate the transport across 24°N to be $1.2 \pm 0.3 \times 10^{15}$ W whereas the model prediction for the mean annual transport across this latitude is 0.55×10^{15} W.

The primary contribution to the heat transport comes from the meridional overturning mode of the circulation. The sensitivity of this aspect of the circulation to various sub-grid scale parameterizations is well-documented in Bryan (1987). The net overturning in the model (Figure 8) is somewhat lower than estimates based on observations. This difference is easily accounted for by the uncertainty in the strength of vertical mixing processes. In this limited area model the specification of the open boundary conditions also affects the total overturning in the basin. While the water mass properties appear to be set correctly in the buffer zones, the exchange of water entering and leaving them appears to be too weak. Thus, while the gain and loss of heat within the basin appear to agree well with observations, the net heat transport through the basin is too small.

The contributions of the mean flow and the eddies to the northward heat transport are shown in Figure 9. The eddy contribution is largest in the latitude band of the Gulf Stream but never exceeds 10% of the contribution of the mean flow. In sharp contrast to the situation in the atmosphere, it appears that transient eddies in the ocean do not make a large direct contribution to the total poleward heat transport.

An Example of Wave-Mean Flow Interaction

The equatorial circulation system in the Atlantic has a large seasonal cycle and is the most energetic part of the basin outside of the Gulf Stream region. The model successfully simulates the seasonal formation of the North Equatorial Counter Current (NECC) during summer and fall as well as the development of "equatorial long waves" (see Philander et al., 1986) on the NECC, as shown in Figure 10. These waves are the result of baroclinic instability and are responsible for the equatorward heat transport between 0° and 10°N seen in Figure 7. Note that the isotherms tilt up towards the equator in this region, so that the eddy heat flux is indeed down gradient.

The circulation in this region is particularly sensitive to variations in the dissipation, and this sensitivity reveals an interesting example of wave-mean flow interaction processes. A one year sensitivity experiment in which the vertical viscosity was reduced from 30 cm^2s^{-1} to 10 cm^2s^{-1} was run starting from the conditions at the begining of year 20 of the standard case. The strength of the Equatorial Undercurrent increased by approximately 50 percent and it penetrated farther to the east. The amplitude of the waves on the NECC also grew significantly, and the wave field penetrated several more wavelengths to the east (Figure 11). Since these eddies are responsible for the equatorward heat transport, we might expect this to increase as well. The maximum magnitude of the total heat transport was essentially the same in the two cases, however.

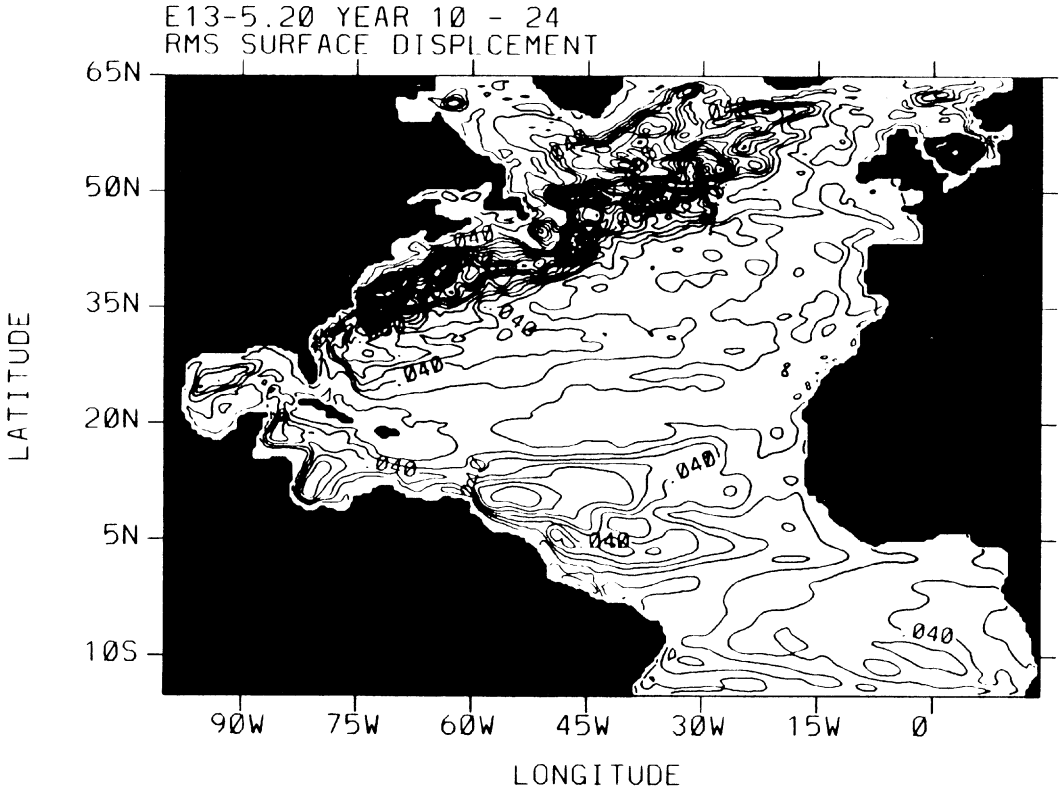

Figure 6. Distribution of standard deviation of sea surface height.

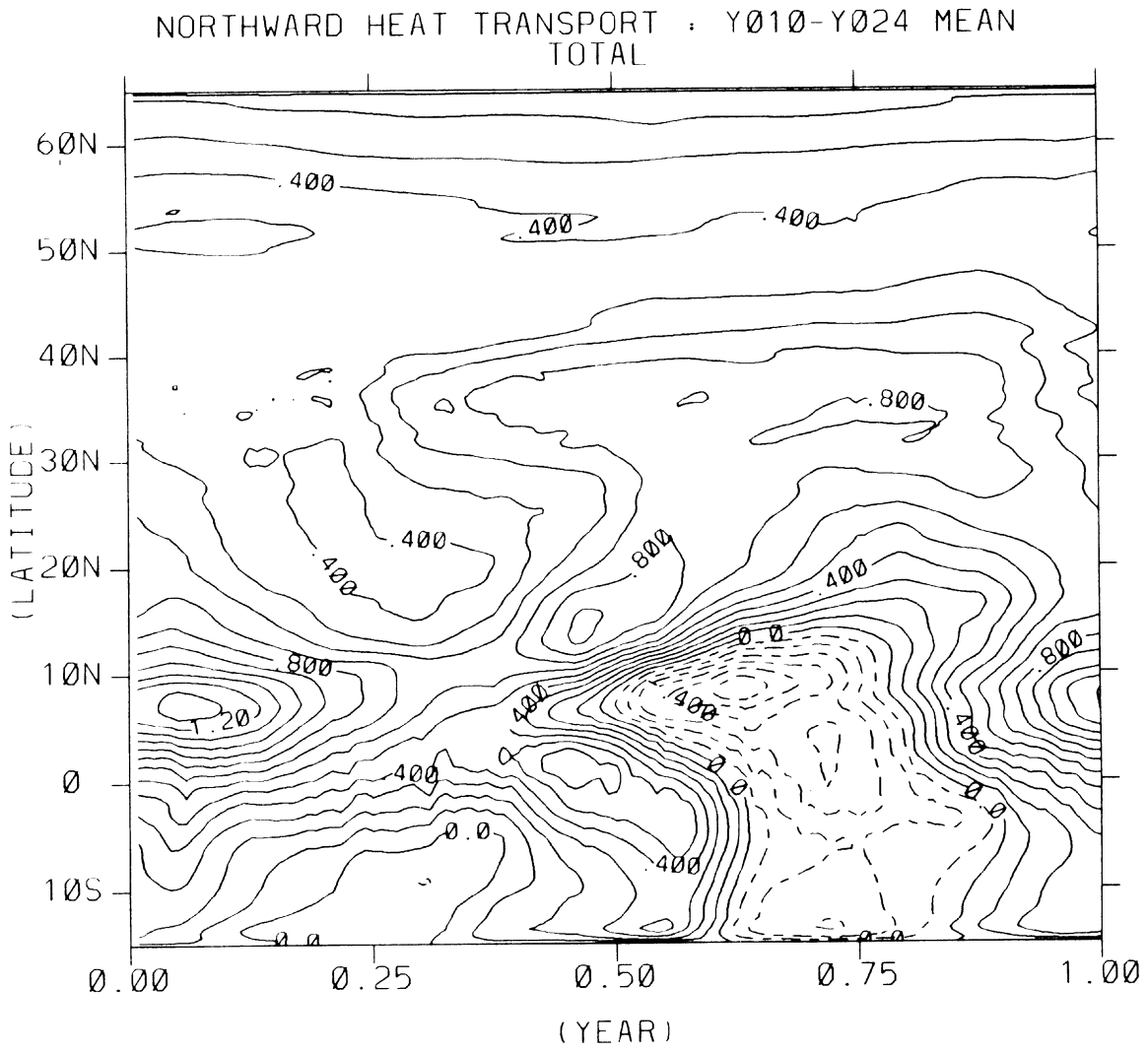

Figure 7. Mean annual cycle of meridional distribution of northward heat transport. Units are 10^{15} W.

The resolution to this paradox is apparent in Figure 12. The southward heat transport by the eddies is opposed by a northward heat transport due to a shallow meridional overturning cell, which is itself partially driven by the eddies (analogous to the Ferrell cell in the atmosphere). In the low dissipation case, the increase in the direct heat transport by the eddies is almost exactly canceled by the changes in the heat transport by the mean flow due to the change in the driving of the mean flow by the eddies. This provides very clear example of strong eddy interactions with a climatically important process.

CONCLUSIONS

The experiment described here represents the current state-of-the-art in ocean general circulation modeling. It is clear that the physical processes responsible for both water mass formation and eddy formation can be successfully simulated in models of this class.

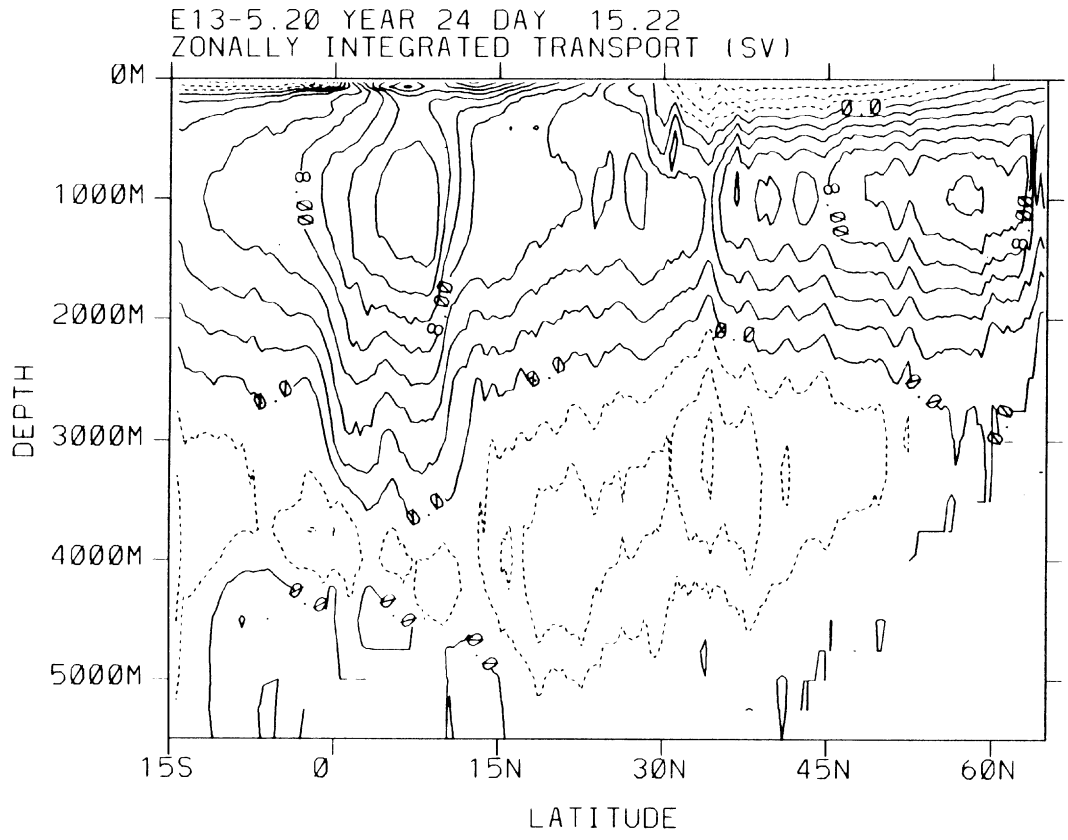

Figure 8. Streamfunction for the zonally integrated transport during mid-January of the final year of the integration.

The major area of difficulty remaining in the model is the simulation of the western boundary current near the separation point. Experience with quasigeostrophic models of the mid-latitude circulation suggest that even higher resolution will be required to overcome these difficulties. We have seen that both the eddies and the mean flow are very sensitive to the magnitude of the dissipation provided by sub-grid-scale parameterizations, and thus many more experiments of this type will be required before we can quantify our confidence in the simulations. Further, as we are now able to explicitly resolve most of the important scales involved in quasigeostrophic eddies, the class of motions that are regarded as "sub-grid-scale" has been redefined. It appears that the next major level of model development should be directed towards improving our understanding and the parameterization of the truly small scale processes responsible for diapycnal mixing and momentum dissipation.

This experiment provides one of the first estimates of the contribution of mesoscale eddies to ocean heat transport. The direct contribution of the eddies to the heat transport was 10% or less of the contribution of the mean flow. In at least one region however, we saw that the eddies had strong interactions with the mean flow itself, and thus strong indirect effects on climatically important aspects of the ocean circulation.

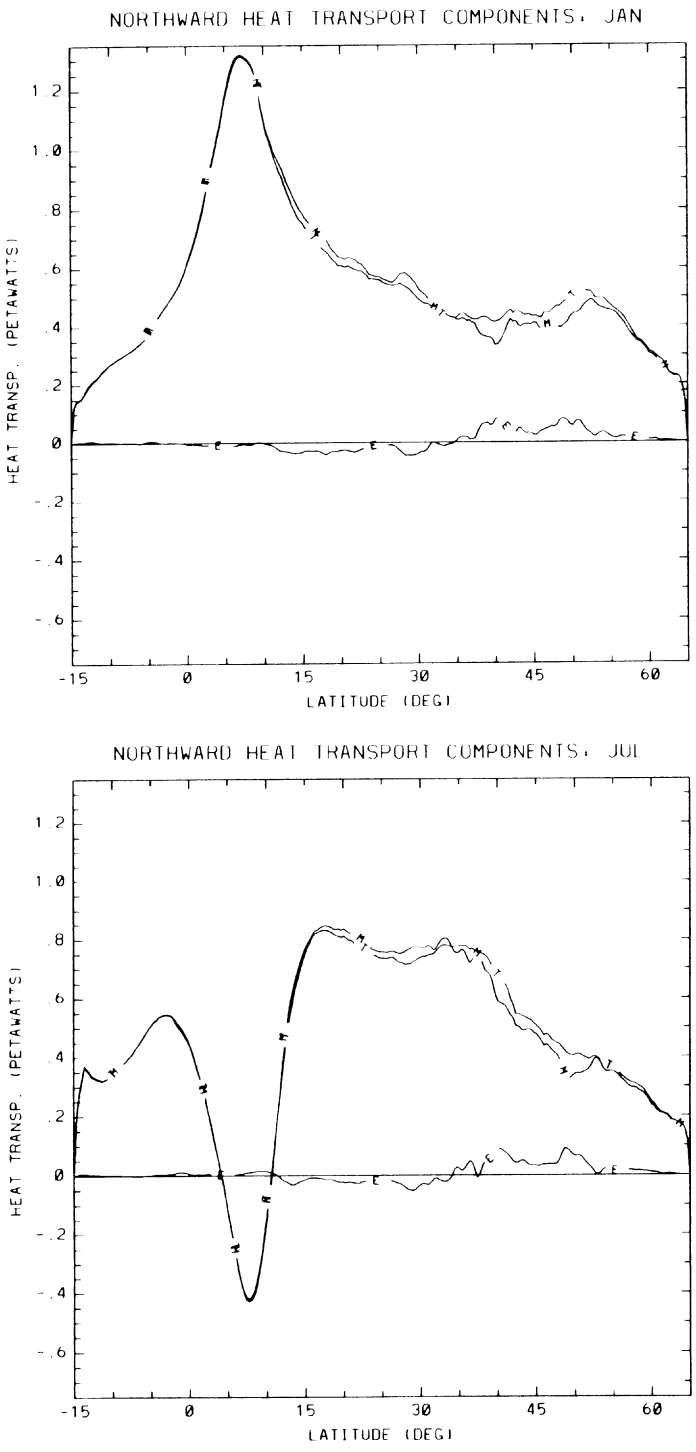

Figure 9. Total heat transport (T), the contribution of the time mean flow to the total heat transport (M), and the eddy contribution to the total heat transport (E) for January (top) and July (bottom).

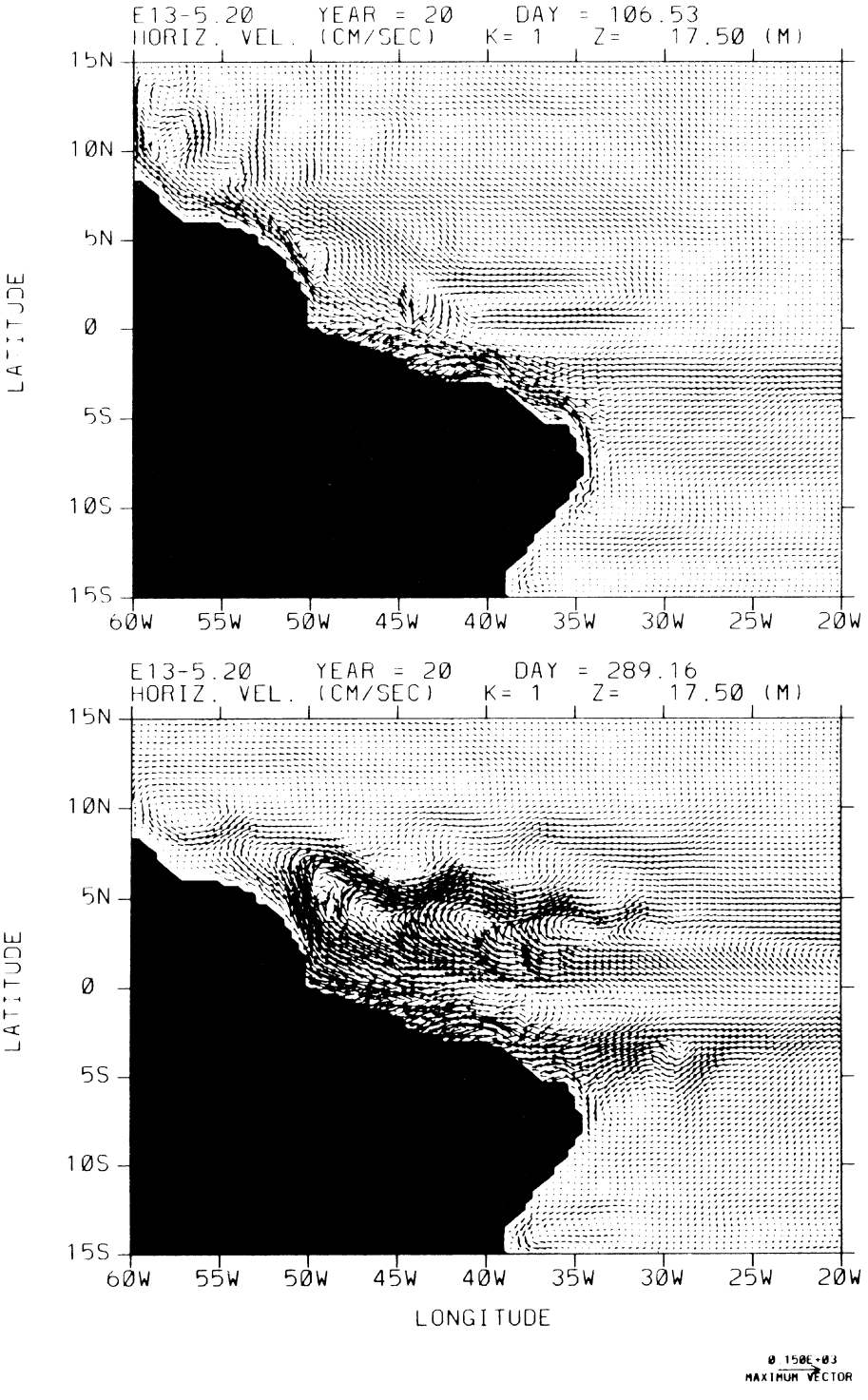

Figure 10. a) Horizontal velocity at 17.5 m in the western equatorial region for mid-April during the year 20 of the standard experiment. Vector in the lower right represents 150 cm s^{-1}. b) As above for mid-October.

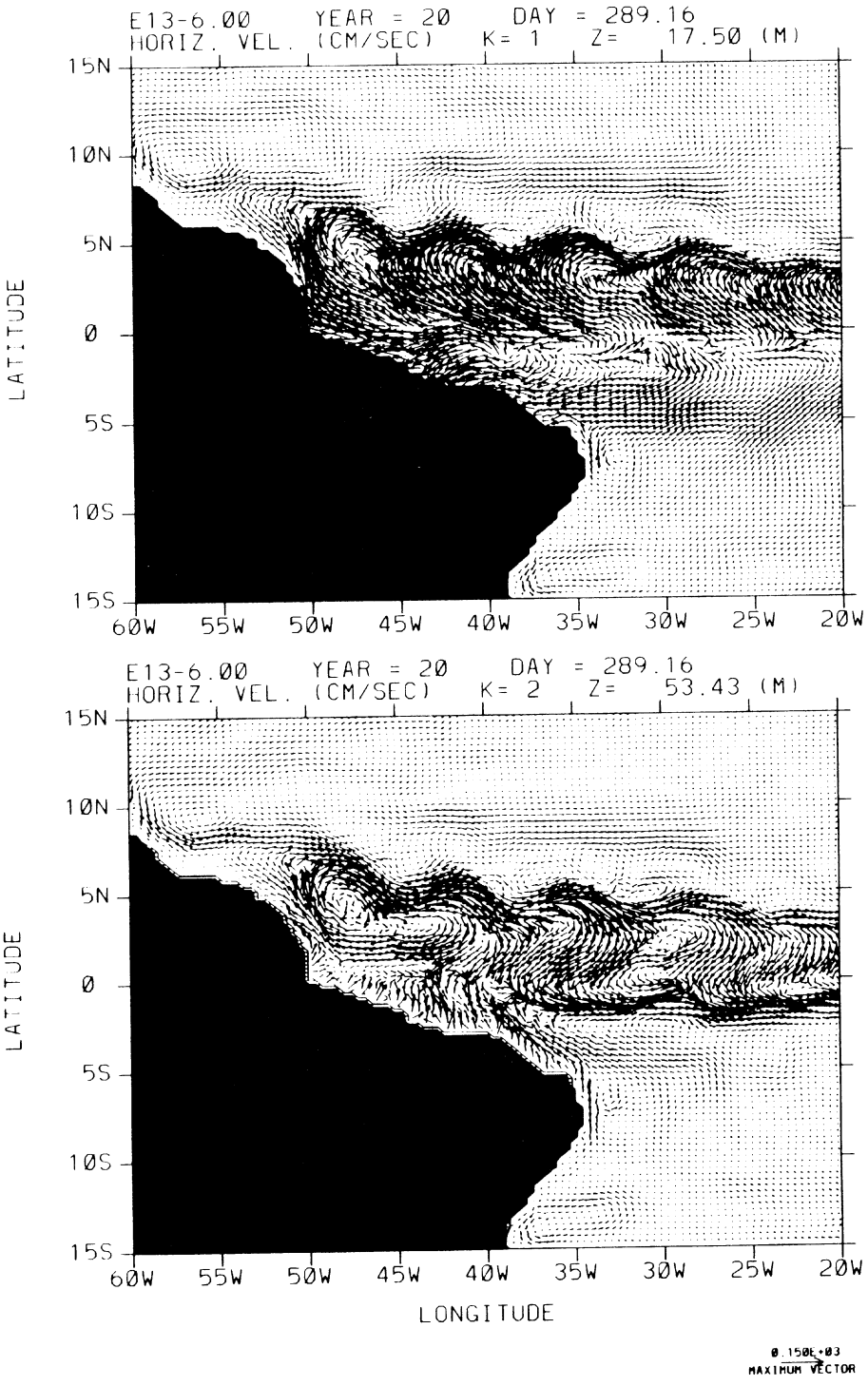

Figure 11. a) Horizontal velocity at 17.5 m in the western equatorial region for mid-October during year 20 of the case with decreased vertical viscosity. Vector in the lower right represents 150 cm s^{-1}. b) As above except at 53.4 m.

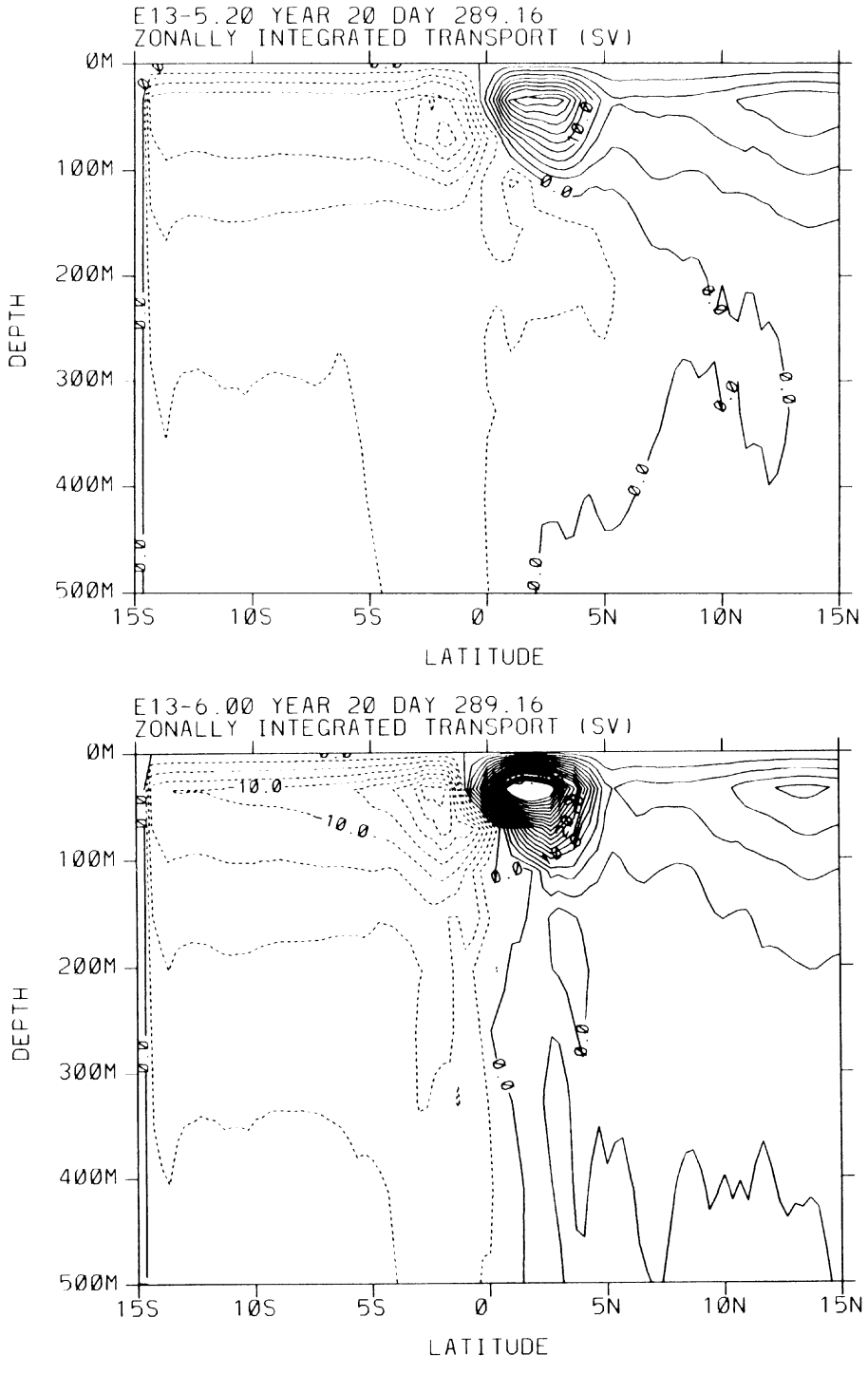

Figure 12. a) Zonally integrated transport in the equatorial region during mid-October for the standard experiment. b) As above for the case with reduced vertical viscosity.

REFERENCES

Arakawa, A. and V.R. Lamb: 1977. Computational design of the basic dynamical processes of the UCLA general circulation model. In: *Methods in Computational Physics*, 17, J. Chang (Ed.), Academic Press.

Bryan, F.: 1987. Parameter sensitivity of primitive equation ocean general circulation models. *J. Phys. Ocean.*, 17, 970-985.

Bryan, K.: 1969. A numerical method for the study of the circulation of the world ocean. *J. Comput. Phys.*, 4, 347-376.

Bryan, K.: 1979. Models of the world ocean circulation. *Dynamics of Atmospheres and Oceans*, 3, 327-338.

Cox, M.D.: 1984. A primitive equation three dimensional model of the ocean. *GFDL Ocean Group Technical Report No. 1*, Geophysical Fluid Dynamics Laboratory/NOAA.

Gill, A.E. and P.P. Niiler: 1973. The theory of the seasonal variability in the ocean. *Deep-Sea Res.*, 20, 141-177.

Hall, M.M. and H.L. Bryden: 1982. Direct estimates and mechanisms of ocean heat transport. *Deep-Sea Res.*, 29, 339-360.

Han, Y.-J.: 1984. A numerical world ocean general circulation model. Part II A baroclinic experiment. *Dynamics of Atmospheres and Oceans*, 8, 141-172.

Hellerman, S. and M. Rosenstein: 1983. Normal monthly wind stress over the world ocean with error estimates. *J. Phys. Oceanogr.*, 13, 1093-1104.

Holland, W.R., D.E. Harrison, and A.J. Semtner, Jr.: 1983. Eddy resolving numerical models of large-scale ocean circulation. In : *Eddies in Marine Science*, A.R. Robinson (Ed.), Springer-Verlag, 379-403.

Holland, W.R.: 1985. Simulation of mesoscale ocean variability in mid-latitude gyres. In: *Issues in Atmospheric and Oceanic Modeling. Part A: Climate Dynamics*, S. Manabe (Ed.) Reviews of Geophysics, 28, Academic Press, 479-523.

Holland, W.R.: 1986. Quasi-geostrophic modelling of eddy-resolved ocean circulation. In: *Advanced Physical Oceanographic Numerical Modeling*, J.J. O'Brien (Ed.), NATO ASI Series C: Mathematical and Physical Sciences, 186, Reidel, 203-231.

Koblinsky, C.: 1988. GEOSAT vs. SEASAT. *EOS Trans. Amer. Geophys. Union*, 69, 1026.

Leaman, K.D., R.L. Molinari, and P.S. Vertes: 1987. Structure and variability of the Florida Current at 27°N : April 1982-July 1984. *J. Phys. Oceanogr.*, 17, 565-583.

Levitus, S.: 1982. Climatological Atlas of the World Ocean, *NOAA Prof. Paper 13*, U.S. Govt. Print. Office. 173 pp.

Meehl, G.A., W.M. Washington, and A.J. Semtner: 1982. Experiments with a global ocean model driven by observed atmospheric forcing. *J. Phys. Oceanogr.*, 12, 301-312.

Philander, S.G.H., W.J. Hurlin, and R.C. Pacanowski: 1986. Properties of long equatorial waves in models of the seasonal cycle in the Tropical Atlantic and Pacific Oceans. *J. Geophys. Res.*, 91, 14207-14211.

Philander, S.G.H., W.J. Hurlin and A.D. Siegel: 1987. Simulation of the seasonal cycle of Tropical Pacific Ocean, *J. Phys. Oceanogr.*, 17, 1986-2002.

Sarmiento, J.L.: 1986. On the North and Tropical Atlantic heat balance, *J. Geophys. Res.*, 91, 11677-11689.